Received 2025; | Revised 2025; | Accepted 2025

DOI: xxx/xxxx

ARTICLE TYPE

Radial Velocity Monitoring and Analysis of Gaia Astrometry of Selected Intermediate Mass Stars to Constrain Their Multiplicity Status

J. Bätz* | M. Mugrauer | K.-U. Michel | J. Reichert | A. Tschirschky | L. Pietsch | F. Edelmann | R. Neuhäuser

Astrophysical Institute and University Observatory, Friedrich-Schiller-University Jena, Schillergäßchen 2, 07745 Jena, Germany

Correspondence
*Janine Bätz. Email: baetz.janine@gmail.com

We present new radial velocity measurements of 13 selected intermediate mass stars (2 – 6 $M_{\odot}$). The measurements were performed between 29 April and 6 September 2024 at the University Observatory Jena using the échelle spectrograph FLECHAS. The radial velocity of eight stars was found to be constant during our spectroscopic monitoring, namely: 17 Dra A, HD 148374, HD 169487 A, 57 Cnc, γ And, HD 11031, κ And, and λ Cas. In contrast, the radial velocity of five stars showed significant variability throughout or spectroscopic observation, namely: 7 CrB A, 7 CrB B, HD 214007, ι Her, and HD 201433 A. In all these cases, Keplerian orbital solutions were fitted to the observational data and the orbital elements of these spectroscopic binary systems were determined. In addition, we searched for wide companions of our targets using the third data release from ESA's Gaia mission, in order to determine the multiplicity status of these stars and contribute to the census of bright, nearby multiple stars.

KEYWORDS:
techniques: radial velocities, methods: observational, binaries: general, binaries: spectroscopic, stars: individual (17 Dra A, HD 148374, HD 169487 A, 57 Cnc, γ And, HD 11031, κ And, λ Cas, 7 CrB A, 7 CrB B, HD 214007, ι Her, HD 201433 A)

1 | INTRODUCTION

In Bätz, Neuhäuser, Hambaryan, and Hambardzumyan (2025) about 600000 stars with absolute magnitudes $M_G \leq 0.65$ mag, located within a radius of 1.7 kpc around the Sun, were retrieved from the third data release of the ESA Gaia mission (Gaia DR3 from here on, see Gaia Collaboration et al., 2023), to detect OB-type runaway stars[1] originating from the Scorpius-Centaurus-Lupus association among them. This sample contains a large number of stars with no known radial velocity (RV) in the Gaia DR3, the Extended Hipparcos Compilation (Anderson & Francis, 2012) or the Simbad database (Wenger et al., 2000), which are however needed to trace their trajectories back in time. In order to obtain at least some additional RV measurements, a subset of these stars was therefore selected for observation at the University Observatory Jena. Since most of the runaway stars are slower than the peak velocities of runaway stars of about 200 km/s (Blaauw, 1961), the most promising runaway star candidates found in (Bätz et al., 2025) were expected to still be located relatively close to the Scorpius-Centaurus-Lupus association. Therefore, only stars within a defined radius of approximately 166 pc around the Sun were considered for observation. This resulted in a subsample of 105 stars, 13 of which can be observed at the University

[1] Unusually fast-moving early-type stars, which have attained their high space velocities either by dynamical ejection or by supernova explosion in multiple star systems.

Observatory Jena. The properties of these targets are summarized in Table 1. It should be noted that the stars presented in this paper were then excluded as runaway stars from the Scorpius-Centaurus-Lupus association according to Bätz et al. (2025) – partly because of the RV measured here. All targets were observed with the échelle spectrograph FLECHAS (Mugrauer, Avila, & Guirao, 2014, Fibre Linked ECHelle Astronomical Spectrograph) operated at the 0.9 m telescope of the University Observatory Jena to determine their RV. For stars whose RV remained constant during the observations, the mean and standard deviation of their RV were calculated and are presented in this paper. For stars with a significantly variable RV, we attempted to fit a best-fitting Keplerian orbital solution to the RV data to determine the orbital elements of these systems, including their systemic velocity.

2 | METHOD

All targets listed in Table 1 were observed with FLECHAS at the University Observatory Jena between 29 April and 6 September 2024. Three spectra were recorded per observation epoch, which were then combined into a fully reduced spectrum during data reduction. Before the actual spectroscopy of each target, three spectra were taken from a bulb lamp for flat-field correction and from a a thorium-argon lamp for wavelength-calibration, respectively. Three spectra of a bulb lamp were recorded before the spectroscopy of each target for flat-field correction, and three spectra of a thorium-argon lamp were taken for wavelength calibration. For dark subtraction, three darks were median combined into a master dark for each detector integration time. The signal-to-noise ratio (SNR) of all fully reduced spectra was measured at a wavelength of 6500 Å. The RV was then determined using the Doppler shift $\Delta\lambda = \lambda - \lambda_0$ of the Hα-line:

$$\mathrm{RV} = c\,\frac{\Delta\lambda}{\lambda_0} + BC \tag{1}$$

where λ is the measured wavelength of the spectral line, λ_0 is the rest wavelength, c is the speed of light and BC is the barycentric correction.

The wavelength of the Hα-line was determined by fitting a Gaussian profile on the Doppler-broadened core of the spectral line using the IRAF (Tody, 1993) task `splot`. The uncertainty of the RV measurements (ΔRV), given below, results from the error in the Gaussian-fitting and in the wavelength calibration. This error can be assumed to be constant for all RV measurements of the same star since we always examined the Hα-line which does not spontaneously change in its width; thus, the error of the RV measurements only depends on the quality of the respective spectra, i.e. the signal-to-noise ratio (SNR). Only negligible variations in the SNR values were observed, justifying the use of a constant ΔRV.

Those stars whose RV remained constant during the given period of observation are presented in Section 3 of this paper. For illustration purposes, their RV is plotted over the barycentric Julian date (BJD), which is given in the format of BJD − 2460000.

Stars with variable RV are discussed in this paper in Section 4. In these cases, a Keplerian orbital solution was fitted to the RV data using the spectroscopic binary solver (Johnson, 2004). The RV of a component of a binary system varies by:

$$\mathrm{RV} = K\,[e\,\cos(\omega) + \cos(\omega + \nu)] + \gamma \tag{2}$$

while the component orbits the barycenter of the system, where K is the RV semi-amplitude, ν is the true anomaly of the component, ω is the argument of periastron, e is the orbital eccentricity and γ is the systemic velocity. K is further given by:

$$K = \frac{2\pi\ a\sin(i)}{P\sqrt{1-e^2}} \tag{3}$$

with the minimum semi-major axis $a\sin(i)$ of the orbit of the component around the barycenter of the system and the orbital period P of the system.

3 | STARS WITH CONSTANT RADIAL VELOCITY

From the sample of stars shown in Table 1, eight were found to have a constant RV during our spectroscopic monitoring. These are: 17 Dra A, HD 148374, HD 169487 A, 57 Cnc A, γ And, HD 11031, κ And, and λ Cas. To determine how well the model of a constant RV matches the RV measurements of an observed target, considering the given measurement uncertainties, we calculated the reduced χ^2-value for each fit, which is defined as follows:

$$\chi^2_{\mathrm{red}} = \frac{1}{n-1}\sum\left(\frac{RV - \overline{RV}}{\Delta RV}\right)^2 \tag{4}$$

Here, n is the number of the individual measurements RV with their typical uncertainty ΔRV, and their mean value $\overline{RV}$.

In addition, a linear function was fitted to the RV measurements of each target to check whether a linear trend in the RV data over time can be detected. If the slope $\frac{\mathrm{dRV}}{\mathrm{dt}}$ of the fitted linear function is not significantly different from zero, this indicates that the RV of the target remained stable during the observation period. The significance of this slope was evaluated using Pearson's test. None of the eight stars presented in the following subsections were found to have a significant linear trend or periodic variation in their RV.

TABLE 1 The observed targets together with their right ascension α, declination δ, apparent G-band brightness, Gaia FLAME mass estimate *mass*, effective temperature $T_{\rm eff}$ and surface gravity log(g), as listed in the Gaia DR3. The geometric distance *dist* of all targets was taken from Bailer-Jones et al. (2021). In addition, the detector integration time (DIT) and the number of observation epochs $N_{\rm Obs}$ are given for each target. The range of $T_{\rm eff}$ of all targets corresponds to spectral types B5 – K0.

Target	α [hh:mm:ss.ss]	δ [dd:mm:ss.s]	G [mag]	*dist* [pc]	*mass* [$M_\odot$]	$T_{\rm eff}$ [K]	$\log(g[{\rm cm/s^2}])$	DIT [s]	$N_{\rm Obs}$
17 Dra A	16 36 13.72	+52 55 27.9	5.402 ± 0.003	$126.79^{+1.44}_{-1.82}$	$3.09^{+0.05}_{-0.04}$	10832^{+56}_{-51}	$3.76^{+0.01}_{-0.01}$	150	16
HD 148374	16 23 47.16	+61 41 47.3	5.807 ± 0.003	$152.16^{+0.86}_{-0.94}$	$3.75^{+0.19}_{-0.04}$	6347^{+122}_{-24}	$2.67^{+0.03}_{-0.01}$	150	17
HD 169487 A	18 22 11.80	+51 32 30.9	6.818 ± 0.003	$158.79^{+0.41}_{-0.51}$	$2.75^{+0.04}_{-0.04}$	10291^{+62}_{-37}	$3.86^{+0.01}_{-0.01}$	300	11
57 Cnc	08 54 14.73	+30 34 44.8	5.774 ± 0.003	$115.21^{+0.91}_{-0.85}$	$2.80^{+0.04}_{-0.04}$	5269^{+272}_{-46}	$2.76^{+0.03}_{-0.04}$	150	10
γ And	02 03 54.76	+42 19 51.3	4.863 ± 0.011	$85.40^{+6.09}_{-6.12}$	$2.62^{+0.09}_{-0.09}$	9611^{+17}_{-16}	$4.02^{+0.03}_{-0.03}$	60	11
HD 11031	01 49 15.53	+47 53 48.9	6.458 ± 0.003	$137.14^{+2.41}_{-2.12}$	$2.72^{+0.05}_{-0.05}$	10407^{+59}_{-45}	$3.88^{+0.01}_{-0.01}$	300	10
κ And	23 40 24.51	+44 20 02.2	4.148 ± 0.003	$51.44^{+0.44}_{-0.60}$	$2.80^{+0.04}_{-0.05}$	11101^{+35}_{-104}	$3.98^{+0.01}_{-0.01}$	60	14
λ Cas	00 31 46.35	+54 31 20.1	4.648 ± 0.004	$137.76^{+13.61}_{-10.50}$	$3.69^{+0.13}_{-0.12}$	11217^{+33}_{-36}	$3.46^{+0.02}_{-0.02}$	60	13
7 CrB A	15 39 22.67	+36 38 08.9	4.985 ± 0.003	$155.55^{+2.22}_{-2.66}$	$3.89^{+0.05}_{-0.05}$	12157^{+34}_{-38}	$3.76^{+0.01}_{-0.01}$	60	30
7 CrB B	15 39 22.24	+36 38 12.6	5.975 ± 0.003	$155.33^{+0.88}_{-0.78}$	$3.60^{+0.05}_{-0.05}$	13292^{+58}_{-74}	$4.04^{+0.01}_{-0.02}$	300	25
HD 214007	22 33 53.15	+61 46 41.3	6.535 ± 0.003	$162.60^{+0.65}_{-0.47}$	$2.37^{+0.04}_{-0.04}$	7907^{+9}_{-9}	$3.46^{+0.01}_{-0.01}$	300	16
ι Her	17 39 27.89	+46 00 22.8	3.791 ± 0.004	$154.11^{+6.07}_{-5.27}$	$5.40^{+0.12}_{-0.08}$	14346^{+104}_{-96}	$3.61^{+0.02}_{-0.02}$	60	38
HD 201433 A	21 08 38.89	+30 12 20.3	5.719 ± 0.003	$121.46^{+1.51}_{-1.34}$	$3.09^{+0.05}_{-0.05}$	11786^{+63}_{-126}	$4.00^{+0.01}_{-0.01}$	150	17

3.1 | 17 Dra A

The Washington Visual Double Star Catalog (WDS from here on, see Mason, Wycoff, Hartkopf, Douglass, & Worley, 2001) lists three companions of 17 Dra (see Table 2 for details). However, of these three stars, only the B and C components could be confirmed as part of the 17 Dra system, as they all have very similar parallaxes and proper motions listed in the Gaia DR3. 17 Dra A itself has a parallax of $\varpi_{\rm A} = 7.89 \pm 0.10$ mas and a proper motion of $\mu^*_{\alpha,{\rm A}} = -12.24 \pm 0.13$ mas/yr and $\mu_{\delta,{\rm A}} = 26.82 \pm 0.16$ mas/yr. The corresponding values of 17 Dra B are and 17 Dra C are: $\varpi_{\rm B} = 7.52 \pm 0.12$ mas, $\mu^*_{\alpha,{\rm B}} = -15.54 \pm 0.17$ mas/yr, $\mu_{\delta,{\rm B}} = 31.48 \pm 0.21$ mas/yr, and $\varpi_{\rm C} = 7.74 \pm 0.09$ mas, $\mu^*_{\alpha,{\rm C}} = -12.78 \pm 0.12$ mas/yr, $\mu_{\delta,{\rm C}} = 27.64 \pm 0.15$ mas/yr. In contrast, the D component from the WDS has a parallax of $\varpi = 3.4 \pm 0.30$ mas and can therefore be excluded as part of the system. In addition to the confirmed WDS components, another companion of 17 Dra A was found in the Gaia DR3. This companion, henceforth referred to as 17 Dra D, is located south of the star ($\theta \sim 189\,°$) at an angular separation of $\rho = 80.7''$ (or $\sim$ 10200 au projected separation). This companion has a parallax of $\varpi = 7.95 \pm 0.05$ mas and a proper motion of $\mu^*_\alpha = -12.53 \pm 0.09$ mas/yr and $\mu_\delta = 27.13 \pm 0.10$ mas/yr, which agree well with the parallax and proper motion of 17 Dar A. Thus, 17 Dra is a hierarchical quadruple system consisting of two binary systems (with projected separations of 390 and 1500 au) separated by about 11000 au.

To quantify the degree of common proper motion (cpm) of all companions directly detected by Gaia, we calculated the cpm-index according as defined by Mugrauer (2019). Additionally, we compared the detected differential proper motion between each companion relative to its primary star with the companion's escape velocity, as estimated by Mugrauer (2019). In the case of the 17 Dra system, the companions detected have cpm-indices of 11, 61 and 138 for 17 Dra B, C, and D respectively, meaning they all exhibit a high degree of cpm with the primary star of the system. Furthermore, the parallaxes of the components do not significantly deviate from each other, and their differential proper motions relative to 17 Dra A do not exceed the estimated escape velocities. This is all as expected for components of a gravitationally bound multiple star system.

TABLE 2 Components of 17 Dra, listed in the WDS, with their angular separation ρ and position angle θ, measured in the first and last observing epoch.

Comp.	Date 1	ρ_1 [$''$]	θ_1 [deg]	Date 2	ρ_2 [$''$]	θ_2 [deg]
B	1781	4.0	114	2022	3.0	104
C	1823	90.3	196	2018	90.2	193
CD	1879	116.9	122	2020	125.5	123

Spectroscopic observations of 17 Dra A were performed with FLECHAS in 16 observation epochs over a period of 79 days. The obtained individual RV measurements of the star

TABLE 3 For 17 Dra A, 16 RV measurements were carried out over a period of 79 days. The typical uncertainty of the RV measurements is $\Delta RV = 1.20$ km/s. The table includes the SNR of all spectra.

BJD − 2460000	RV [km/s]	SNR
430.48932	−14.47	180
432.41889	−12.95	164
439.45953	−14.92	187
444.44487	−13.55	176
445.43250	−15.14	162
446.38934	−14.51	128
451.37339	−15.86	172
468.48837	−16.87	170
469.50364	−14.86	161
473.52038	−14.49	137
481.49545	−15.93	139
486.39842	−13.49	191
487.39599	−13.13	177
501.47496	−16.70	179
508.47437	−14.25	145
509.51423	−15.87	122

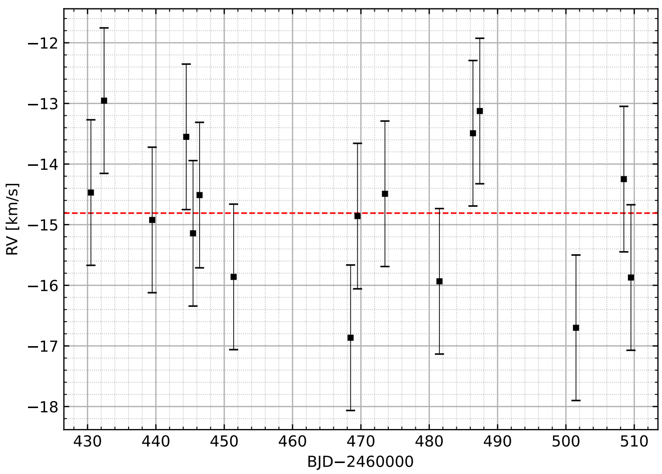

FIGURE 1 The RV of 17 Dra A measured over a period of 79 days. The mean RV is indicated by the dashed red line.

are summarized in Table 3. As illustrated in Figure 1, the RV of the star is constant during the entire spectroscopic observation time.

3.2 | HD 148374

The WDS lists **two** components for HD 148374, which are summarized in Table 4. The Ab component is not detected by Gaia due to its small angular separation of only 0.2″ (or about 30 au projected separation), as expected from the direct imaging performance of Gaia, determined by Mugrauer, Kollak, Pietsch, and Michel (2025). In contrast, an object is listed near the position of the B component in the Gaia DR3 ($\rho \sim 0.858''$ and $\theta \sim 359.1°$), but neither parallax nor proper motion are given for this source. If this object is the same source that is listed for the first observation epoch in the WDS, due to the Gaia DR3 proper motion of HD 148374 ($\mu^*_{\alpha,A} = -29.26 \pm 0.051$ mas/yr and $\mu_{\delta,A} = 35.25 \pm 0.06$ mas/yr) and the long epoch difference of 184 years between the first WDS and the Gaia observation (reference epoch 2016.0) this object must be a true companion of the star. If this source discovered in 1832 were a background star, it would have to be located at $\rho \sim 7.8''$ and $\theta \sim 136°$ in 2016, i.e. at a significantly different position than listed in the Gaia DR3. In contrast, the observed change in position angle of 8° between the first WDS and the Gaia observation epoch is well compatible with the orbital motion in 184 years expected for such a companion at a projected separation of about 140 au. Since the status of the nearby component Ab is not yet clear, we classify HD 148374 as the main component of a binary star system.

TABLE 4 Components of HD 148374, listed in the WDS, with their angular separation ρ and position angle θ, measured in the first and last observing epoch.

Comp.	Date 1	ρ_1 [″]	θ_1 [deg]	Date 2	ρ_2 [″]	θ_2 [deg]
Ab	1986	0.2	174	1990	0.2	154
B	1832	0.9	7	2021	0.9	350

A total of 17 RV measurements of HD 148374 were carried out with FLECHAS over a period of 79 days. All these measurements are listed in Table 5 and plotted in Figure 2. No significant RV variation of the star was detected during our entire spectroscopic monitoring program of the star.

3.3 | HD 169487 A

HD 169487 has no entries in the WDS. However, the star has a very wide ($\rho \sim 315''$ or about 50200 au projected separation) companion in the Gaia DR3, which is about 9 mag fainter in the G-band than HD 169487. Therefore, we classify HD 169487 as the primary component of a wide binary system and will therefore be referred to as HD 169487 A from here on. HD 169487 A has a parallax of $\varpi_A = 6.2801 \pm 0.0203$ mas and a proper motion of $\mu^*_{\alpha,A} = 15.905 \pm 0.025$ mas/yr and $\mu_{\delta,A} = -12.879 \pm 0.027$ mas/yr. The detected companion has a parallax of $\varpi_B = 6.2809 \pm 0.0253$ mas and

TABLE 5 For HD 148374, 17 RV measurements were carried out over a period of 79 days. The typical error of each RV measurement is $\Delta RV = 0.23$ km/s. The table includes the SNR of all spectra.

BJD − 2460000	RV [km/s]	SNR
430.47855	−23.10	192
432.38072	−23.66	177
439.45192	−23.33	197
443.46678	−23.58	139
444.43428	−23.49	172
445.42352	−23.38	180
446.38157	−23.51	131
450.47754	−23.66	172
468.48009	−23.15	191
469.49589	−23.68	181
473.51291	−23.72	160
481.48415	−23.64	224
486.38958	−23.18	206
487.38728	−23.89	197
501.46656	−23.41	192
508.46658	−23.60	152
509.50457	−23.82	158

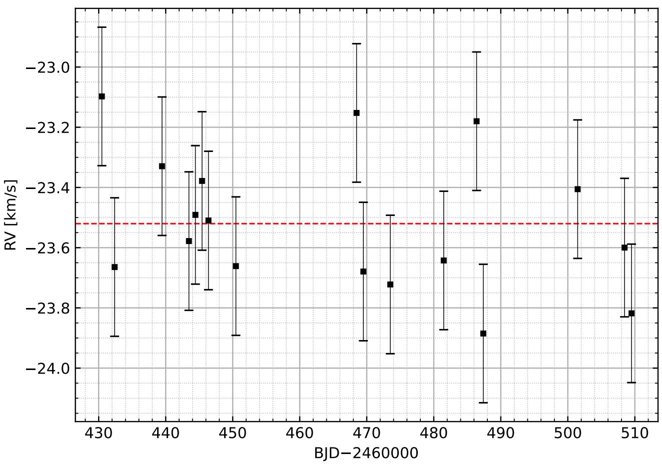

FIGURE 2 The RV of HD 148374 measured over a period of 79 days. The mean RV is indicated by the dashed red line.

a proper motion of $\mu^*_{\alpha,\mathrm{B}} = 16.337 \pm 0.032$ mas/yr and $\mu_{\delta,\mathrm{B}} = -12.247 \pm 0.029$ mas/yr. Gaia DR3 astrometry proves that HD 169487 A and B are equidistant, as their parallaxes do not significantly deviate from each other. The companion has a cpm-index of 53, meaning the two components of this star system exhibit a high degree of common proper motion. However, it should be noted that the companion's differential proper motion to its primary is approximately 1.6 times greater than its estimated escape velocity. Since it is very unlikely that a binary star system would be observed during a destructive event, the higher differential proper motion could suggest the presence of another close companion around one of the components of the system. Such a close companion with its rapid orbital motion leads to a shift in the star's photocenter, which can induce an increased differential proper motion.

The RV of HD 169487 A was monitored with FLECHAS in 11 observation epochs over a period of 91 days. The RV of the star was constant during our entire spectroscopic observation campaign, as shown in Table 6 and Figure 3.

TABLE 6 For HD 169487 A, 11 RV measurements were carried out over a period of 91 days. The typical error of each RV measurement is $\Delta RV = 0.35$ km/s. The table includes the SNR of all spectra.

BJD − 2460000	RV [km/s]	SNR
430.50341	4.14	117
439.47117	3.53	126
443.48021	3.41	95
445.46825	3.76	112
451.44839	4.17	132
459.44927	3.66	95
468.53879	4.30	120
469.47046	3.80	116
486.50704	3.65	139
501.52976	4.59	131
521.47611	4.28	99

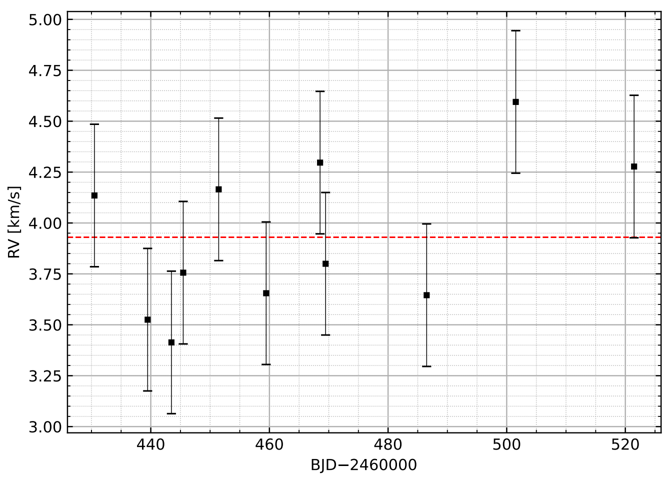

FIGURE 3 The RV of HD 169487 A measured over a period of 91 days. The mean RV is indicated by the dashed red line.

3.4 | 57 Cnc

57 Cnc is listed in the WDS as a hierarchical triple star system (see Table 7).

TABLE 7 Components of 57 Cnc, listed in the WDS, with their angular separation ρ and position angle θ, measured in the first and last observing epoch.

Comp.	Date 1	ρ_1 [″]	θ_1 [deg]	Date 2	ρ_2 [″]	θ_2 [deg]
B	1782	0.9	338	2019	1.5	310
AB, C	1921	55.8	198	2015	54.6	204

However, only the B component can be confirmed as a true companion of the star, as it has a Gaia DR3 parallax and proper motion similar to those of 57 Cnc A:
$\varpi_A = 8.64 \pm 0.07$ mas, $\varpi_B = 8.61 \pm 0.06$ mas
$\mu^*_{\alpha,A} = 41.21 \pm 0.08$ mas/yr, $\mu_{\delta,A} = -23.25 \pm 0.06$ mas/yr
$\mu^*_{\alpha,B} = 37.55 \pm 0.05$ mas/yr, $\mu_{\delta,B} = -24.89 \pm 0.06$ mas/yr.
The companion has a cpm-index of 23, hence is clearly co-moving with 57 Cnc A. In addition, the differential proper motion of the companion to 57 Cnc A is smaller than its estimated escape velocity as expected for a gravitationally bound companion.
In contrast, the C component listed in the WDS has a cpm index of only 0.5, and hence can clearly be ruled out as a co-moving companion of 57 Cnc A. Furthermore, the Gaia DR3 parallax $\varpi = 1.96 \pm 0.02$ mas of this star is very different from that of 57 Cnc A and B, which clearly disqualifies it as part of the 57 Cnc system. Since no other companions of the star were found in the Gaia DR3, 57 Cnc is a binary system with a projected separation of about 180 au and not a triple star system as suggested in the WDS.

The RV of 57 Cnc, was measured in our spectroscopic monitoring program in ten observation epochs over a period of 36 days and proved to be stable within this span of time. All individual RV measurements of the star are listed in Table 8 and plotted in Figure 4.

TABLE 8 For 57 Cnc ten RV measurements were carried out over a period of 36 days. The typical error of each RV measurement is $\Delta RV = 0.30$ km/s. The table includes the SNR of all spectra.

BJD − 2460000	RV [km/s]	SNR
432.35093	−57.63	177
439.36150	−57.71	187
443.35848	−57.32	172
444.34824	−57.19	179
445.34874	−57.46	180
446.34396	−57.77	128
450.39132	−58.10	150
456.36031	−57.94	156
459.35548	−57.89	147
468.37627	−57.79	126

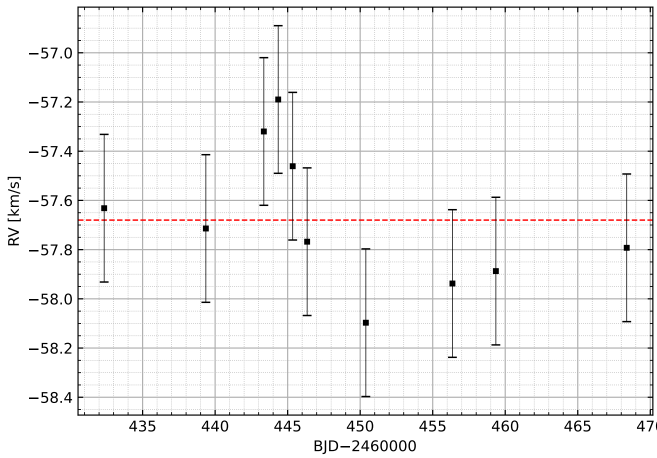

FIGURE 4 The RV of 57 Cnc measured over a period of 36 days. The mean RV is indicated by the dashed red line.

3.5 | γ And

For γ And three components are listed in the WDS (see Table 9) but none of these stars are detected by Gaia. No other companions of the star are listed in the Gaia DR3. Since the angular separation and position angle of the BC component has not changed much with 244 years of epoch difference between the first and the last WDS observation, we conclude that it is a true companion of γ And with a projected separation to the star of about 1000 au.

If this close pair of stars discovered in 1777 were a background source with negligible proper motion in 2021 it would have to be located at $\rho \sim 18''$ and $\theta \sim 23°$ according to the Gaia DR3 proper motion of γ And ($\mu^*_{\alpha,A} = 16.645 \pm 0.930$ mas/yr, $\mu_{\delta,A} = -47.746 \pm 0.90$ mas/yr) and the long epoch difference of 244 years, but this differs significantly from the position, measured in the last WDS observation epoch. For this close binary system an orbital period of about 63 years was derived, as reported in the 6th Catalog of Orbits of Visual Double Stars (Hartkopf, Mason, & Worley, 2001). Furthermore, according to the WDS, the B component is itself a spectroscopic binary with a period of about 2.7 days. In contrast, the status of the D component listed in the WDS is ambiguous, as its detection was reported for only one observation epoch, and no source is listed near its position in the Gaia DR3. From this we conclude that γ And is the primary component of a hierarchical quadruple system.

TABLE 9 Components of γ And, listed in the WDS, with their angular separation ρ and position angle θ, measured in the first and last observing epoch.

Comp.	Date 1	ρ_1 [″]	θ_1 [deg]	Date 2	ρ_2 [″]	θ_2 [deg]
BC	1777	12.0	67	2021	9.5	63
D	1898	27.9	245	–	–	–

γ And was observed with FLECHAS in 11 observation epochs within a monitoring period of 44 days, but no significant variation in its RV was detected.

TABLE 10 For γ And, eleven RV measurements were carried out over a period of 44 days. The typical error of each RV measurement is ΔRV = 0.60 km/s. The table includes the SNR of all spectra.

BJD − 2460000	RV [km/s]	SNR
516.56282	−8.55	536
520.54226	−8.32	715
531.52621	−7.90	606
533.46280	−7.88	680
535.57245	−7.10	782
538.51730	−7.55	700
545.50779	−7.30	552
549.56800	−6.78	645
550.54184	−6.58	729
555.44836	−7.53	625
560.50345	−8.11	521

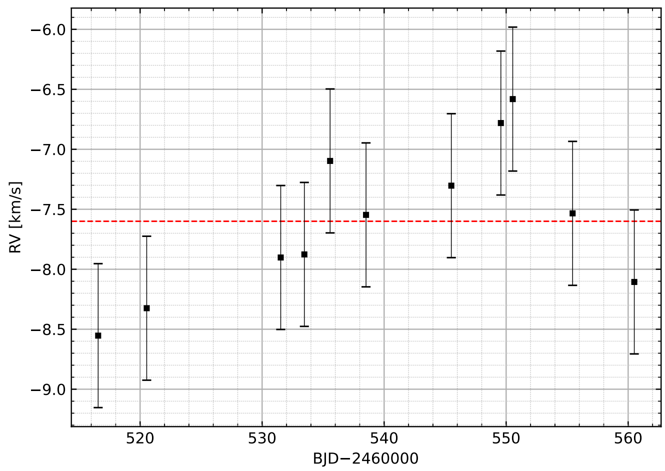

FIGURE 5 The RV of γ And measured over a period of 44 days. The mean RV is indicated by the dashed red line.

3.6 | HD 11031

HD 11031 is listed in the WDS as a multiple star system (see Table 11). The companionship of the B and C components to HD 11031 A can be confirmed with their Gaia DR3 astrometry due to comparable parallaxes ($\varpi_A = 7.29 \pm 0.12$ mas, $\varpi_B = 6.44 \pm 0.17$ mas, $\varpi_C = 7.76 \pm 0.03$ mas) and proper motions:
$\mu^*_{\alpha,A} = -16.92 \pm 0.15$ mas/yr, $\mu_{\delta,A} = -2.85 \pm 0.10$ mas/yr
$\mu^*_{\alpha,B} = -15.45 \pm 0.17$ mas/yr, $\mu_{\delta,B} = -9.18 \pm 0.10$ mas/yr
$\mu^*_{\alpha,C} = -20.38 \pm 0.04$ mas/yr, $\mu_{\delta,C} = -9.53 \pm 0.03$ mas/yr.
In contrast, the D component listed in the WDS can clearly be excluded as a companion of the star, as it has a cpm-index of only 0.5 and its Gaia DR3 parallax ($\varpi = 2.89 \pm 0.03$ mas) is significantly different from that of HD 11031 A. Based on the Gaia DR3 astrometry, the projected separation between HD 11031 A & B is about 270 au, and ∼2800 au between HD 11031 A & C. Due to its small angular separation of only 0.1″, the Ab component is not listed in the Gaia DR3, but its companionship to HD 11031 is proven, as an orbital solution with a period of about 37 yr could be derived for this star, as reported in the WDS. This catalog also mentions that HD 11031 B itself is a spectroscopic double star, i.e. HD 11031 is actually a quintuple star system. Components B and C have cpm-indices of about 5, meaning they share a common proper motion with HD 11031 A. However, the 5-parameter astrometric solution of the individual components of the HD 11031 system show large astrometric excess noises of 0.836, 0.897, and 0.198 mas for HD 11031 A, B, and C. Taking these noises into account, the parallaxes of the components agree with each other; that is to say, these stars are equidistant, as would be expected of gravitationally bound members of a star system. While the differential proper motion of HD 11031 B to the primary star is smaller than its estimated escape velocity, that of HD 11031 C is about 3.1 greater than the escape velocity estimated for this star. As described above, this high differential proper motion could be caused by a close companion of the star that has not been detected. In this context, it is worth noting that all components of the HD 11031 system also have a high Renormalized Unit Weight Error (RUWE): 4.12 for HD 11031 A, 4.56 for HD 11031 B, and 1.78 for HD 11031 C. This suggests the possible presence of additional close companions of these stars. While such companions are already known orbiting HD 11031 A and HD 11031 B, RUWE = 1.78 for HD 11031 C could indicate that also this star might harbor

an additional close companion (see e.g. Castro-Ginard et al., 2024, and references therein), which would also explain the higher differential proper motion observed for this star.

TABLE 11 Components of HD 11031, listed in the WDS, with their angular separation ρ and position angle θ, measured in the first and last observing epoch.

Comp.	Date 1	ρ_1 [″]	θ_1 [deg]	Date 2	ρ_2 [″]	θ_2 [deg]
Ab	1984	0.1	194	1994	0.1	251
B	1828	2.2	227	2020	2.0	197
C	1828	20.6	177	2020	20.7	178
D	1881	134.7	95	2016	138.8	96

The RV of HD 11031 was monitored over a period of 44 days in ten observing epochs, but no significant RV variation was detected. The RV measurements of the star are summarized in Table 12 and are plotted in Figure 6.

TABLE 12 For HD 11031, ten RV measurements were carried out over a period of 44 days. The typical error of each RV measurement is $\Delta RV = 0.60$ km/s. The table includes the SNR of all spectra.

BJD – 2460000	RV [km/s]	SNR
516.54405	−4.61	141
520.56169	−4.06	162
528.58723	−4.99	151
534.51877	−4.01	151
538.50813	−3.87	179
545.49812	−5.32	138
549.51387	−5.16	164
550.53126	−4.73	187
555.43879	−3.59	152
560.48008	−4.40	142

3.7 | κ And

The WDS lists multiple components for κ And, which are summarized in Table 13. However, components B and C can be ruled out as real companions of the star, since both stars only have small cpm-indices of about 0.9 and their Gaia DR3 parallaxes ($\varpi < 1.0$ mas) differ greatly from that of κ And ($\varpi = 19.41 \pm 0.21$ mas). In contrast, the companion listed at an angular separation of about 1″ (or about 50 au of projected

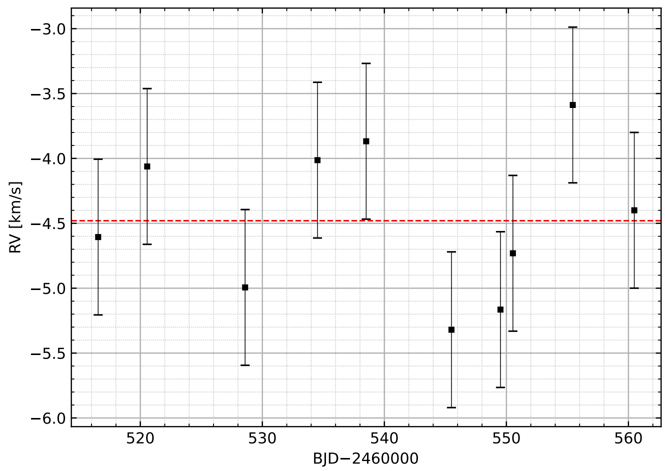

FIGURE 6 The RV of HD 11031 measured over a period of 44 days. The mean RV is indicated by the dashed red line.

separation) is of substellar nature and is in fact part of the system (Carson et al., 2013). No additional companions of the star are detected in the Gaia DR3.

TABLE 13 Components of κ And, listed in the WDS, with their angular separation ρ and position angle θ, measured in the first and last observing epoch.

Comp.	Date 1	ρ_1 [″]	θ_1 [deg]	Date 2	ρ_2 [″]	θ_2 [deg]
Ab	2011	1.1	56	2012	1.0	51
B	1828	35.0	182	2002	47.4	202
C	1836	98.5	296	2012	115.3	293

κ And was observed with FLECHAS in 14 observing epochs distributed over a period of 114 days, during which time the RV of the star remained stable. All measurements are displayed in Table 14 and plotted in Figure 7.

3.8 | λ Cas

According to the WDS, λ Cas is a binary system (see Table 15) for which a premature orbital solution with a period of about 246 years was determined by Drummond (2014).

A total of 13 RV measurements were carried out for λ Cas with FLECHAS over a period of 44 days. The star's individual RV measurements are listed in Table 16 and shown in Figure 8. No significant RV variability was observed during the entire observation period.

TABLE 14 For κ And, 14 RV measurements were carried out over a period of 114 days. The typical error of each RV measurement is $\Delta RV = 1.90$ km/s. The table includes the SNR of all spectra.

BJD – 2460000	RV [km/s]	SNR
445.55471	−20.27	124
451.52514	−21.40	163
516.53550	−17.62	253
520.53391	−17.04	332
522.56758	−18.39	211
531.51545	−17.43	256
533.45423	−18.25	215
535.50917	−17.81	215
538.49901	−20.27	198
545.48871	−22.34	174
549.45990	−17.41	177
550.47650	−20.27	72
555.42770	−20.69	303
559.47165	−16.29	113

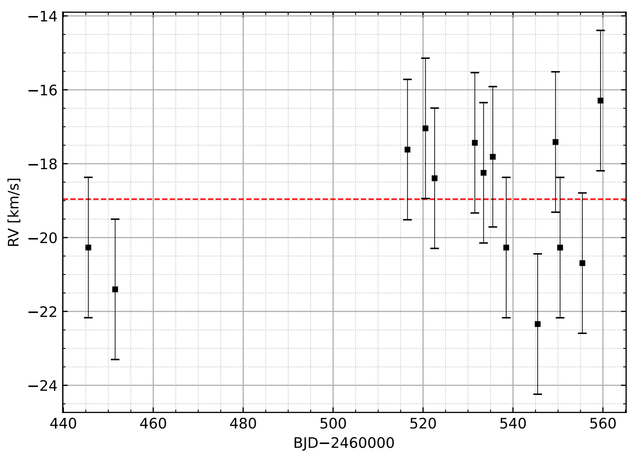

FIGURE 7 The RV of κ And measured over a period of 114 days. The mean RV is indicated by the dashed red line.

TABLE 15 Components of λ Cas, listed in the WDS, with their angular separation ρ and position angle θ, measured in the first and last observing epoch.

Comp.	Date 1	ρ_1 [″]	θ_1 [deg]	Date 2	ρ_2 [″]	θ_2 [deg]
B	1845	0.3	122	2020	0.2	239

3.9 | Summary

Table 17 summarizes the results for the targets presented in the previous subsections. All of these stars showed a constant RV during our spectroscopic monitoring program, which was performed with FLECHAS at the University Observatory Jena. The table lists the mean and standard deviation of the RV measurements for each star, as well as the $\chi^2_{\rm red}$-value of the fits to the RV data for these stars, assuming RV = const. As the $\chi^2_{\rm red}$-value of all fits is around one, the RV measurements of all targets are consistent with a constant RV within their uncertainties.

TABLE 16 For λ Cas, 13 RV measurements were carried out over a period of 44 days. The typical error of each RV measurement is $\Delta RV = 2.90$ km/s. The table includes the SNR of all spectra.

BJD – 2460000	RV [km/s]	SNR
516.55504	−17.07	111
520.53863	−15.36	156
522.57169	−24.15	160
531.52078	−16.36	224
533.45677	−17.11	151
535.51261	−21.54	163
538.50164	−15.73	148
542.58402	−22.13	154
545.49174	−17.43	132
549.46305	−21.14	123
550.47951	−22.75	141
555.43250	−19.00	145
560.43533	−19.63	129

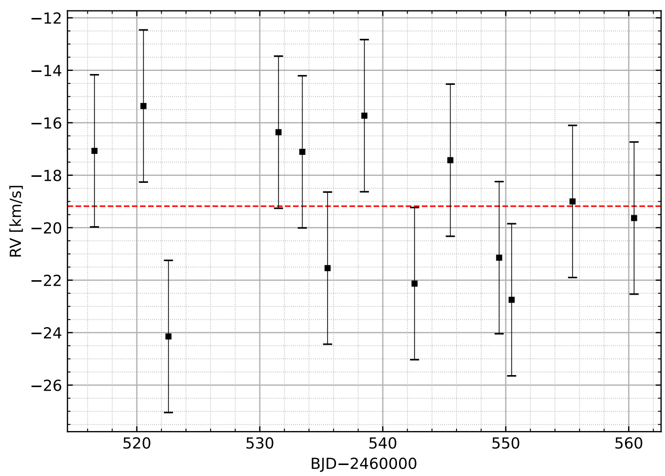

FIGURE 8 The RV of λ Cas measured over a period of 44 days. The mean RV is indicated by the dashed red line.

TABLE 17 List of all stars that have a constant RV in our spectroscopic monitoring program with FLECHAS. For each target, we list the mean and standard deviation of its RV, as well as the $\chi^2_{\rm red}$-value of the fit assuming a constant RV.

Target	$\overline{\rm RV}$ [km/s]	$\chi^2_{\rm red}$
17 Dra A	-14.81 ± 1.20	1.00
HD 148374	-23.52 ± 0.23	1.01
HD 169487 A	3.93 ± 0.39	1.17
57 Cnc	-57.68 ± 0.28	0.90
γ And	-7.60 ± 0.63	1.09
HD 11031	-4.48 ± 0.59	0.95
κ And	-18.96 ± 1.86	0.96
λ Cas	-19.18 ± 2.92	1.01

4 | STARS WITH VARIABLE RADIAL VELOCITY

Of the total sample of targets shown in Table 1, five stars exhibit significant variability in their RV measurements. Keplerian orbital solutions were fitted to the RV data for all these targets to determine the orbital elements of these spectroscopic binary systems. In order to accurately determine these elements, it is important to obtain a sufficiently large number of RV measurements that cover the system's orbital phase adequately. The $\chi^2_{\rm red}$-value is given for all best-fitting Keplerian orbital solutions, as a measure of how well these solutions agree with the RV measurements, taking into account their uncertainties. All targets, with variable RV, are discussed in more detail in separate subsections below.

For single-lined spectroscopic binaries (SB1) their mass function:

$$f(m) = \frac{\left(mass_2\ \sin i\right)^3}{\left(mass_1 + mass_2\right)^2} = \frac{K^3\ P\ (1-e^2)^{3/2}}{2\pi G} \qquad (5)$$

was determined, where $mass_1$ is the mass of the observed star, $mass_2$ the mass of the spectroscopically detected companion, and G the gravitational constant. In addition, also the minimum semi-major axis:

$$a \sin i = \frac{K\ P\ (1-e^2)^{1/2}}{2\pi}. \qquad (6)$$

of the orbit of the observed star around the barycenter of the binary system, was derived.

For double-lined spectroscopic binaries (SB2) the minimum semi-major axes of the orbits of both of their components around the common barycenter were calculated using Equation 6. Furthermore, the minimum mass of these stars:

$$mass_{1/2} \sin^3 i = \frac{(1-e^2)^3/2P}{2\pi G} K_{2/1}(K_1 + K_2)^2 \qquad (7)$$

was determined.

4.1 | 7 CrB A

This star is listed in the WDS as the primary component of a wide binary system (see Table 18). The Gaia DR3 astrometry of 7 CrB A and B confirms the companionship of these two stars as they have similar parallaxes ($\varpi_{\rm A} = 6.43 \pm 0.10$ mas, and $\varpi_{\rm B} = 6.41 \pm 0.05$ mas) and proper motions ($\mu^*_{\alpha,{\rm A}} = -15.51 \pm 0.09$ mas/yr, $\mu_{\delta,{\rm A}} = -7.47 \pm 0.12$ mas/yr, $\mu^*_{\alpha,{\rm B}} = -14.01 \pm 0.04$ mas/yr, $\mu_{\delta,{\rm B}} = -3.92 \pm 0.05$ mas/yr). 7 Crb B has a cpm-index of about 8 and the differential proper motion of the companion to 7 CrB A is smaller than its estimated escape velocity. Further companions of 7 CrB A are not listed in the Gaia DR3. Thus 7 CrB A and 7 CrB B (see also next subsection) form a binary system with a projected separation of about 990 au.

TABLE 18 Components of 7 CrB A, listed in the WDS, with their angular separation ρ and position angle θ, measured in the first and last observing epoch.

Comp.	Date 1	ρ_1 [$''$]	θ_1 [deg]	Date 2	ρ_2 [$''$]	θ_2 [deg]
B	1779	5.5	296	2024	6.3	306

7 CrB A itself is an SB2 system, and a clear splitting of the absorption lines is present in most of the FLECHAS spectra of the star. A total of 30 RV measurements of the two components of the 7 CrB A system were taken over a period of 129 days. The individual RV measurements of the two stars are listed in Table 19. For this target, it proved difficult to find a good Keplerian orbit solution. As shown in the upper panel of Figure 9, the RV measurements of both components still scatter strongly around the found best-fitting orbital solution. The orbit fit for 7 CrB Aa has $\chi^2_{\rm red} = 6.45$, the one for 7 CrB Ab even $\chi^2_{\rm red} = 8.89$, so both are not well-fitting orbital solutions. Therefore, we examined the residuals (O–C) of the determined orbit fits in detail, which are shown in the middle panel of Figure 9. The residuals show a significant linear trend in the form:

$${\rm RV}_{\rm trend} = A + B \times ({\rm BJD} - 2460000) \qquad (8)$$

with the intercept $A = 120.9 \pm 10.2$ km/s and the slope $B = -0.24 \pm 0.02$ (km/s)/day. This trend in the RV residuals clearly indicates the presence of an additional companion revolving around the spectroscopic binary on a wide (few au) orbit. Thus, 7 CrB A is indeed a hierarchical triple star system.

To accurately determine the orbital elements of 7 CrB Aa and Ab, the determined trend was then subtracted from the original RV data of the two components, using the RV in the middle of the observation period (BJD = 501.44716) as a reference. This removed most of the RV scatter, as shown in Figure 9. The orbital fits of the trend-corrected RV data have $\chi^2_{\mathrm{red}} = 1.08$ for 7 Crb Aa, and $\chi^2_{\mathrm{red}} = 1.21$ for 7 CrB Ab, i.e. the derived Keplerian orbital solutions are now both in good agreement with the given RV measurements.

In the orbit fitting of the trend-corrected RV data, all Keplerian orbital elements were initially left unconstrained as usual, resulting in an orbit solution that does not differ significantly from a circular one ($e = 0.00^{+0.02}_{-0.00}$). We therefore set $e = 0$ and then use $\omega_{\mathrm{Aa}} = 0\,^\circ$ and $\omega_{\mathrm{Ab}} = 180\,^\circ$.

The elements of the final orbital solution for 7 CrB Aa and Ab are summarized in Table 26. The best-fitting Kepler orbit obtained implies a minimum semi-major axis and mass:
$a \sin i = 2.98 \pm 0.05\ \mathrm{R}_\odot$, $m \sin^3 i = 0.537 \pm 0.006\ \mathrm{M}_\odot$
for 7 CrB Aa and
$a \sin i = 3.16 \pm 0.05\ \mathrm{R}_\odot$, $m \sin^3 i = 0.505 \pm 0.006\ \mathrm{M}_\odot$
for 7 CrB Ab, respectively.

4.2 | 7 CrB B

As described in the previous section, 7 CrB B is a wide companion of the spectroscopically detected hierarchical triple star system 7 CrB A.

The RV of 7 CrB B was monitored with FLECHAS in 25 observation epochs within a period of 125 days. The individual RV measurements of the star are listed in Table 20. As in the case of 7 CrB A, also 7 CrB B shows a significant RV variation over time.

A Keplerian orbital solution could be fitted to the FLECHAS RV data of 7 CrB B, which agrees well with the RV measurements ($\chi^2_{\mathrm{red}} = 1.03$). The elements of this solution are summarized in Table 26 . The solution presented here implies a minimum semi-major axis of the orbit of the primary component around the barycenter of the system $a \sin i = 0.49 \pm 0.10\ \mathrm{R}_\odot$, and a mass function of the system $f(m) = (9.31 \pm 5.53) \times 10^{-5}\ \mathrm{M}_\odot$.

Hence, 7 CrB is a quintuple star system composed of the spectroscopically identified triple star system 7 CrB A (see previous section), which is orbited by the SB1 system 7 CrB B on a wide orbit with a projected separation of about 990 au.

4.3 | HD 214007

HD 214007 is not listed in the WDS and no companions of the star can be found in the Gaia DR3. The RV of the star was measured 16 times with FLECHAS during an observation time of 130 days. The individual RV measurements are listed in Table 21 and show a considerable variation. Therefore, we have tried to fit a Keplerian orbital solution to the RV data. The best Kepler fit is shown in Figure 11 and agrees well ($\chi^2_{\mathrm{red}} = 1.05$) with the RV data. The Keplerian elements of this solution are listed in Table 26. According to this fit, the orbit of the primary component around the barycenter of the system has a minimum semi-major axis $a \sin i = 9.39 \pm 0.67\ \mathrm{R}_\odot$ and the mass function of the system is $f(m) = 0.11 \pm 0.02\ \mathrm{M}_\odot$.

TABLE 19 For 7 CrB A, 30 RV measurements were carried out over a period of 129 days. The measurements scatter strongly around the best-fitting Keplerian orbital solution, due to a superimposed linear trend in the RV, which was subsequently subtracted from the measurements ($\mathrm{RV_{corr}}$). The typical error of each RV measurement of the Aa component is $\Delta\mathrm{RV} = 4.10$ km/s, or $\Delta\mathrm{RV} = 6.00$ km/s for the Ab component. The table contains the SNR of all spectra.

BJD − 2460000	$\mathrm{RV}^{(\mathrm{Aa})}$ [km/s]	$\mathrm{RV}^{(\mathrm{Aa})}_{\mathrm{corr}}$ [km/s]	$\mathrm{RV}^{(\mathrm{Ab})}$ [km/s]	$\mathrm{RV}^{(\mathrm{Ab})}_{\mathrm{corr}}$ [km/s]	SNR
430.47210	61.82	44.66	−87.32	−104.49	126
432.36450	69.70	52.99	−102.38	−119.09	105
439.37463	65.95	50.94	−95.71	−110.72	123
443.37099	−80.76	−94.80	59.21	45.17	113
444.36213	66.92	53.12	−105.11	−118.91	110
445.36038	−97.67	−111.23	73.31	59.75	123
446.35807	52.51	39.19	−84.85	−98.17	126
450.40350	−99.65	−111.99	71.97	59.63	115
468.37669	47.84	39.85	−92.62	−100.62	120
469.40618	−107.11	−114.86	71.87	64.12	122
481.41943	−109.16	−114.00	65.02	60.18	142
486.40871	−82.40	−86.04	38.10	34.47	134
487.41902	52.26	48.87	−113.20	−116.59	108
501.44716	44.92	44.92	−113.23	−113.23	108
520.35736	40.77	45.34	−128.79	−124.22	114
520.40604	38.38	42.97	−122.14	−117.56	104
520.49585	26.41	31.01	−105.38	−100.77	138
531.33562	−121.02	−113.79	39.46	46.69	108
533.33468	−116.86	−109.15	36.40	44.11	146
533.38321	−109.92	−102.20	32.60	40.32	138
533.43252	−103.15	−95.41	23.80	31.53	123
534.33443	8.26	16.21	−99.18	−91.23	119
538.32875	−127.33	−118.41	45.43	54.35	122
538.37742	−125.50	−116.57	46.08	55.01	109
538.44230	−123.29	−114.34	42.39	51.34	109
545.31564	−125.56	−114.95	45.10	55.71	104
549.30932	15.69	27.26	−100.43	−88.86	96
550.38204	−121.59	−109.76	47.06	58.89	59
555.31172	−90.93	−77.91	17.06	30.08	130
559.31557	−93.26	−79.27	20.35	34.34	110

4.4 | ι Her

The WDS lists two companions of this star (see Table 22), neither of which can be confirmed with astrometric data from the Gaia DR3. The Ab component, whose angular distance to ι Her corresponds to a projected separation of about 30 au, is too close to the star to be listed in the Gaia DR3. Since only one

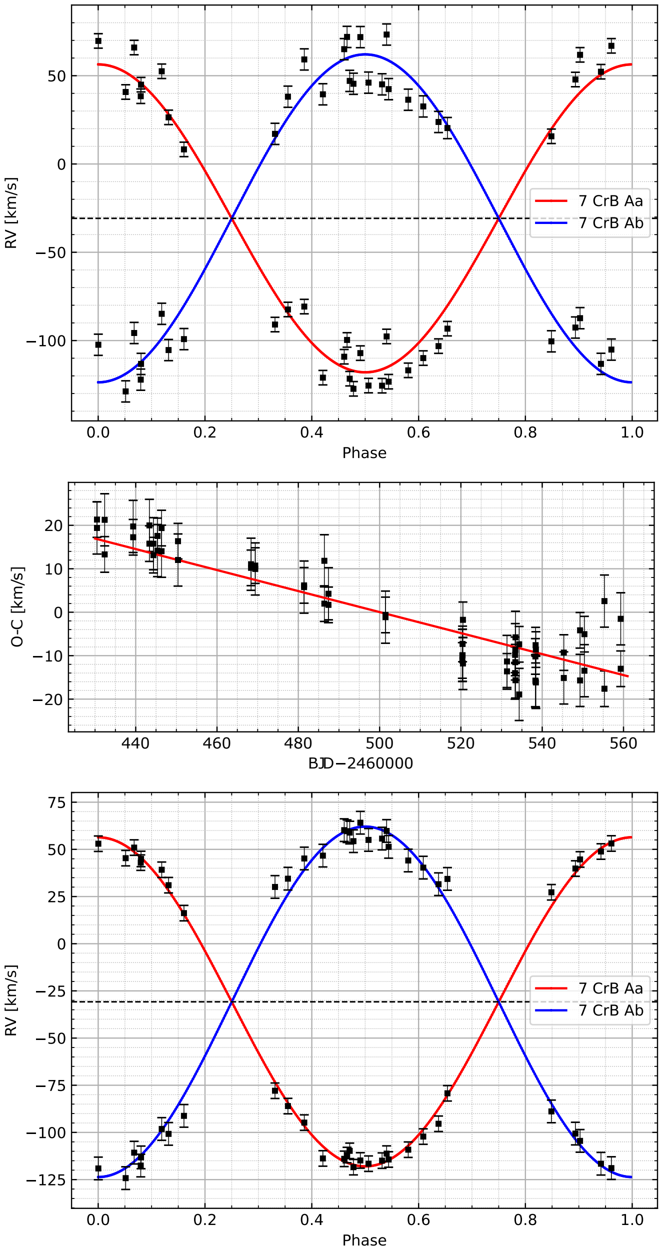

FIGURE 9 **Top panel:** Preliminary orbital fit for 7 CrB Aa (red) and 7 CrB Ab (blue), which still shows a large scattering. **Central panel:** A linear trend (red line; see Equation (8) for the exact function) was observed in the RV residuals of 7 CrB Aa and Ab. **Bottom panel:** The trend-corrected RV data and the best-fitting Keplerian orbital solution for 7 CrB Aa (red) and 7 CrB Ab (blue). The systemic velocity is indicated by the dashed black line. The orbital period is $P = 1.7236 \pm 0.0002$ days.

observational epoch of this component is given in the WDS, its companion status remains inconclusive. The proposed B component is detected in the Gaia DR3, but only has a cpm-index of about 0.9 and a parallax ($\varpi = 1.22 \pm 0.01$ mas) that

TABLE 20 For 7 CrB B, 25 RV measurements were carried out over a period of 125 days. The typical error of each RV measurement is ΔRV = 2.70 km/s. The table includes the SNR of all spectra.

BJD − 2460000	RV [km/s]	SNR
430.46621	−16.78	103
432.37206	−21.08	151
439.38085	−17.33	165
443.37700	−16.27	139
444.36890	−25.59	90
445.36646	−23.91	152
446.36633	−13.73	128
450.40960	−12.82	150
468.39258	−22.07	158
469.41232	−21.83	169
473.43221	−27.21	150
486.41554	−21.11	192
487.42517	−10.88	170
501.45444	−22.11	159
516.43550	−14.94	125
520.36338	−9.49	170
531.34189	−15.00	142
533.34071	−16.88	209
535.34299	−13.02	187
538.33470	−28.21	196
545.32218	−19.40	150
547.39155	−19.91	141
549.31554	−18.57	142
550.38982	−20.96	145
555.31787	−19.13	177

differs significantly from that of ι Her ($\varpi = 6.52 \pm 0.20$ mas). Therefore, this component can be clearly ruled out as a true companion of the star. Further companions of ι Her are not listed in the Gaia DR3.

For ι Her, a total of 38 RV measurements were carried out with FLECHAS over a period of 130 days. They are all summarized in Table 23. The Keplerian orbit solution fitted to these RV data points is shown in Figure 12 and the corresponding orbital elements are listed in Table 26. With these elements we derived the minimum semi-major axis of the orbit of the primary componet of the system $a \sin i = 12.68 \pm 0.74\,R_\odot$ as well as the mass function of the system $f(m) = (2.20 \pm 0.43) \times 10^{-3}\,M_\odot$.

4.5 | HD 201433 A

Three potential companions are listed in the WDS for HD 201433, which are summarized in Table 24.

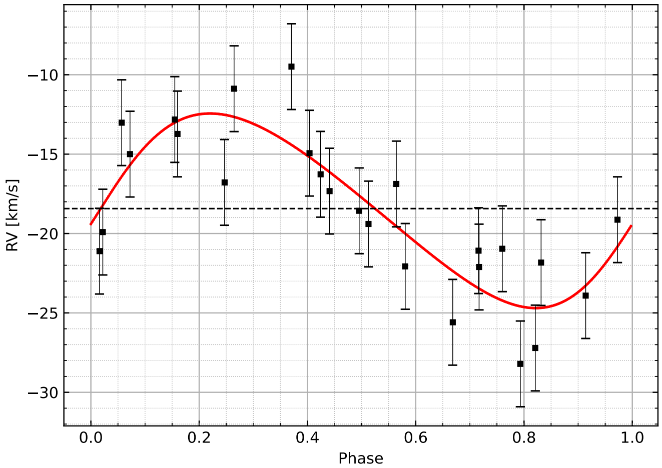

FIGURE 10 The best-fitting Keplerian orbital solution (red line) of the FLECHAS RV data of 7 CrB B with a period of $P = 4.06 \pm 0.01$ days. The systemic velocity is indicated by the dashed black line.

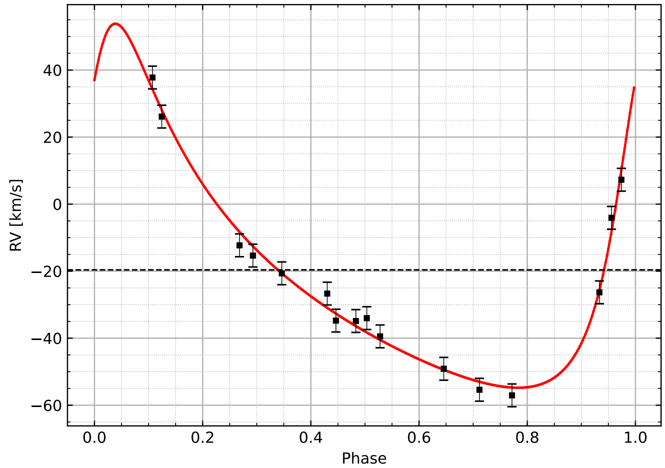

FIGURE 11 Best-fitting Keplerian orbital solution (red line) on the FLECHAS RV data of HD 214007, which has a period of $P = 10.16 \pm 0.01$ days. The systemic velocity is indicated by the dashed black line.

TABLE 21 For HD 214007, 16 RV measurements were carried out over a period of 130 days. The typical error of each RV measurement is $\Delta\mathrm{RV} = 3.40$ km/s. The table includes the SNR of all spectra.

BJD − 2460000	RV [km/s]	SNR
430.51326	−49.13	94
439.48140	−39.46	124
445.54396	26.11	117
451.51301	−55.39	104
469.52137	−34.88	112
516.52393	37.77	119
520.55057	−34.02	151
528.57551	−15.36	121
533.44334	−57.06	171
535.49831	7.27	130
538.48836	−12.30	155
545.47773	−4.09	135
549.44824	−20.65	143
550.46464	−34.76	167
555.41571	−26.32	144
560.46614	−26.70	110

TABLE 22 Components of ι Her, listed in the WDS, with their angular separation ρ and position angle θ, measured in the first and last observing epoch.

Comp.	Date 1	ρ_1 [″]	θ_1 [deg]	Date 2	ρ_2 [″]	θ_2 [deg]
Ab	1975	0.2	6	–	–	–
B	1893	115.1	49	2023	117.2	48

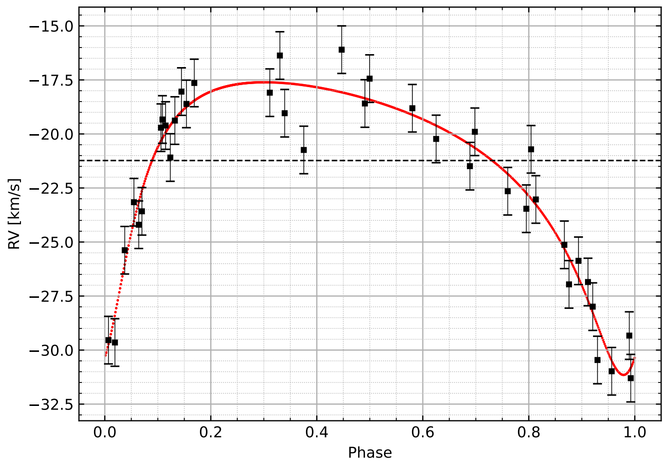

FIGURE 12 Fitted Keplerian orbital solution for ι Her, which has a period of $P = 111.5 \pm 0.1$ days. The systemic velocity is indicated by the dashed black line.

However, only the B component, which has a projected separation of about 410 au to HD 201433, can be confirmed as a true companion of the star, as its Gaia DR3 parallax and proper motion ($\varpi = 8.45 \pm 0.03$ mas, $\mu^*_{\alpha,\mathrm{B}} = 24.00 \pm 0.02$ mas/yr, $\mu_{\delta,\mathrm{B}} = -25.16 \pm 0.03$ mas/yr) are well comparable to those of HD 201433 A ($\varpi = 8.20 \pm 0.10$ mas, $\mu^*_\alpha = 24.65 \pm 0.08$ mas/yr, and $\mu_\delta = -20.65 \pm 0.10$ mas/yr. HD 201433 B has a cpm-index of about 15, and the differential proper motion of the companion to HD 201433 A is smaller than its estimated escape velocity. Components C

TABLE 23 For ι Her, 38 RV measurements were carried out over a period of 130 days. The typical error of each RV measurement is $\Delta RV = 1.10$ km/s. The table includes the SNR of all spectra.

BJD − 2460000	RV [km/s]	SNR
430.49612	−29.33	207
432.42794	−29.54	196
439.46529	−23.58	225
443.47412	−19.71	176
444.45129	−19.61	197
445.43843	−21.09	197
446.39566	−19.38	147
450.48479	−17.64	199
466.37568	−18.09	227
468.49466	−16.37	212
469.51033	−19.04	206
473.52672	−20.74	167
481.50329	−16.10	298
486.38542	−18.59	216
487.38395	−17.44	239
496.37381	−18.81	194
501.38235	−20.23	236
508.48438	−21.49	297
509.52354	−19.90	206
516.44620	−22.65	161
520.35464	−23.46	200
521.35658	−20.71	216
522.35895	−23.03	259
528.35530	−25.13	171
529.34059	−26.96	216
531.33324	−25.87	175
533.33090	−26.85	269
534.33147	−27.99	218
535.33285	−30.46	201
538.32610	−30.98	241
542.33106	−31.30	155
545.31240	−29.65	215
547.37931	−25.38	202
549.30699	−23.16	228
550.32532	−24.20	249
555.30984	−19.33	238
559.31321	−18.04	219
560.35906	−18.61	189

TABLE 24 Components of HD 201433, listed in the WDS, with their angular separation ρ and position angle θ, as measured in the first and last observing epoch.

Comp.	Date 1	ρ_1 [″]	θ_1 [deg]	Date 2	ρ_2 [″]	θ_2 [deg]
B	1783	4.0	315	2020	3.3	303
C	1865	57.7	225	2021	59.0	229
D	1894	74.2	69	2002	73.1	66

and D, on the other hand, can both be excluded as companions of HD 201433 A, as they have a cpm-index of only 0.9 and 1.4, respectively. Furthermore, their parallax ($\varpi_C = 1.27 \pm 0.01$ mas, $\varpi_D = 1.75 \pm 0.03$ mas) differs significantly from that of the star. Further companions of HD 201433 A are not listed in the Gaia DR3.

For HD 201433 A, a total of 17 RV measurements were performed with FLECHAS over a period of 115 days, which are summarized in Table 25. We have fitted a Keplerian orbit solution to all these data, which is shown in Figure 13.

TABLE 25 For HD 201433 A, 17 RV measurements were carried out over a period of 115 days. Measurements that deviate significantly from the orbital solution, considering all RV data, which is shown in Figure 13, are written in gray. The typical error of each RV measurement is $\Delta RV = 2.20$ km/s. The table also contains the SNR of all spectra.

BJD − 2460000	RV [km/s]	SNR
445.50990	−19.13	94
451.47733	−3.38	100
486.54315	−40.14	151
500.54992	−3.65	111
508.52379	−17.35	109
516.45563	−31.87	102
520.51409	5.67	145
528.54257	−24.72	108
531.47316	−11.15	153
533.40637	−25.57	161
535.45312	−42.90	149
538.42472	−26.02	154
545.39957	−40.91	132
549.41059	−46.00	108
550.43157	−12.14	148
555.40373	−40.42	130
560.44223	−14.16	111

As can be seen in Figure 13, some RV measurements scatter significantly around the orbital solution presented

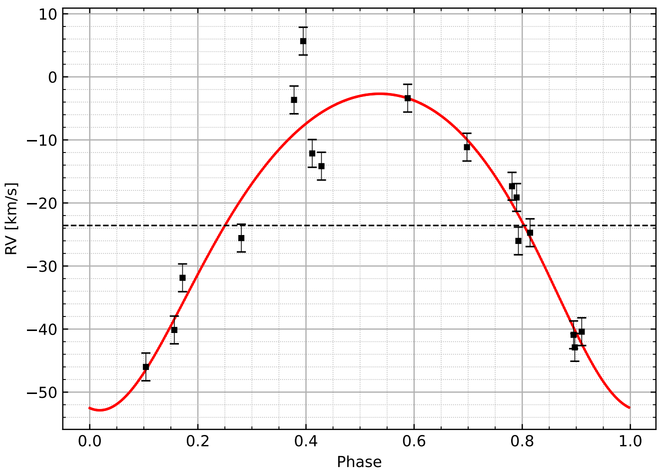

FIGURE 13 Preliminary Keplerian orbit fitted to all RV measurements of HD 201433 A. The derived orbital solution has period of $P = 3.318 \pm 0.004$ days. The systemic velocity is indicated by the dashed black line.

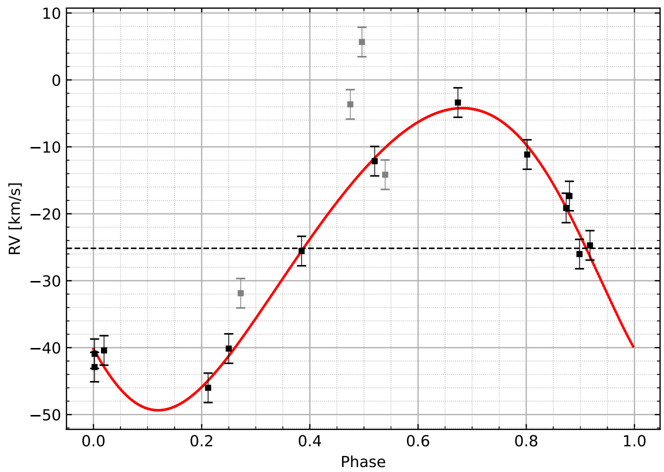

FIGURE 14 Keplerian orbit solution fitted on all RV data of HD 201433 A, with identified outliers (marked in gray) excluded from the fit. This orbital solution has a period of $P = 3.325^{+0.001}_{-0.002}$ days.

($\chi^2_{\mathrm{red}} = 7.78$). Therefore, as already done for 7 CrB A (see Section 4.1), we subtracted the derived Keplerian orbital solution from the RV measurements to examine the residuals for a possible linear trend that could explain the large deviation of some RV measurements from the orbit fit. However, no significant trend could be detected in the RV residuals. So there must be another reason for the RV scattering. In this context, it is worth mentioning that the large RV scattering of the star is also noted in the 9th Catalog of Spectroscopic Double Star Orbits (SB9 from here on, Pourbaix et al., 2004), where it is suggested that both components of HD 201433 A could be pulsating variables.

Assuming that this is true, we attempted to find a better-fitting orbital solution by excluding from the fit all RV measurements that deviate by more than 3σ from the orbital fit based on all RV measurements. The derived elements of both orbital solutions, which do not differ significantly from each other, are listed in Table 26. The resulting final orbital solution ($\chi^2_{\mathrm{red}} = 1.05$) is shown in (Figure 14). From this orbital fit, we obtained $a \sin i = 1.47 \pm 0.08\,\mathrm{R}_\odot$ for the minimum semi-major axis of the primary of the binary system and $f(m) = (3.86 \pm 0.61) \times 10^{-4}\,\mathrm{M}_\odot$ for its mass-function. Thus, HD 201433 is at least a hierarchical triple star system consisting of the SB1 system HD 201433 A, which is orbited by the distant companion HD 201433 B.

4.6 | Summary

For all stars with significant RV variation identified in our RV monitoring program, the elements and the χ^2_{red}-value of the best-fitting Kepler orbital solution are summarized in Table 26.

5 | CONCLUSIONS

For this study, we used FLECHAS at the University Observatory Jena to observe 13 selected stars and accurately determine their mean RV.

The RV of 17 Dra A (RV = -14.81 ± 1.20 km/s) remained constant during our 79-day RV observing program of the star. Therefore, very close companions of 17 Dra A can be excluded. However, according to information from the WDS and Gaia DR3, 17 Dra is actually a hierarchical quadruple system consisting of two binary stars separated by about 11000 au, with projected separations of 390 and 1500 au, respectively.

In order to determine the nature of the detected companions we derived the absolute magnitude and intrinsic color for all components of the 17 Dra system using their Gaia DR3 photometry as well as the reddening and parallax of 17 Dra A. We combined our results with those listed for the components in the VizieR database. We plotted all components of the 17 Dra system in a $(BP - RP)_0$-M_G color-magnitude diagram, which is shown in Figure 15. In this diagram, we also show as gray lines isochrones for stars of solar metallicity and ages of 270 and 310 Myr from the PARSEC 1.2S models[2] (Bressan et al., 2012; Chen et al., 2015, 2014; Marigo et al., 2017; Pastorelli et al., 2020, 2019; Tang et al., 2014), as well as tracks of DA white dwarfs (blue lines) with masses of 0.6, 0.7, and 0.8 $\mathrm{M}_\odot$ from the Bergeron et al. evolutionary white dwarf models[3] (version 2021.01.13, Bédard, Bergeron,

[2] The models are available online at: `https://stev.oapd.inaf.it/PARSEC/`

[3] The models are available online at: `https://www.astro.umontreal.ca/~bergeron/CoolingModels/`

TABLE 26 Elements and $\chi^2_{\rm red}$-value of the best-fitting Kepler orbital solutions determined for all targets that showed significant variation in their RV during our FLECHAS spectroscopy monitoring campaign. In the case of HD 201433 A, two solutions are given. The one written in black considers all RV data, the one written in gray excludes some outliers (see Section 4.5 for more details).

Target	P [d]	T [BJD − 2460000]	e	ω [deg]	K [km/s]	γ [km/s]	$\chi^2_{\rm red}$
7 CrB Aa	$1.7236^{+0.0002}_{-0.0002}$	$428.92^{+0.01}_{-0.01}$	0 (fixed)	0 (fixed)	$87.19^{+1.10}_{-1.09}$	$-30.79^{+0.66}_{-0.66}$	1.08
7 CrB Ab	$1.7236^{+0.0002}_{-0.0002}$	$428.92^{+0.01}_{-0.01}$	0 (fixed)	180 (fixed)	$92.86^{+1.09}_{-1.09}$	$-30.79^{+0.66}_{-0.66}$	1.21
7 CrB B	$4.06^{+0.01}_{-0.01}$	$429.46^{+0.14}_{-0.14}$	$0.16^{+0.14}_{-0.16}$	$262.2^{+66.1}_{-55.1}$	$6.1^{+0.8}_{-0.8}$	$-18.43^{+0.50}_{-0.51}$	1.03
HD 214007	$10.16^{+0.01}_{-0.01}$	$423.95^{+0.11}_{-0.11}$	$0.51^{+0.03}_{-0.03}$	$313.7^{+4.4}_{-4.7}$	$54.3^{+3.8}_{-2.8}$	$-19.62^{+1.22}_{-1.23}$	1.05
ι Her	$111.5^{+0.1}_{-0.1}$	$320.13^{+1.33}_{-1.33}$	$0.53^{+0.03}_{-0.03}$	$208.3^{+5.2}_{-5.0}$	$6.8^{+0.4}_{-0.3}$	$-21.23^{+0.20}_{-0.20}$	1.15
HD 201433 A	$3.318^{+0.004}_{-0.004}$	$442.89^{+0.29}_{-0.29}$	$0.17^{+0.11}_{-0.10}$	$170.5^{+34.5}_{-39.2}$	$25.1^{+3.2}_{-2.7}$	$-23.57^{+1.47}_{-1.66}$	7.78
HD 201433 A	$3.325^{+0.001}_{-0.002}$	$442.61^{+0.16}_{-0.16}$	$0.12^{+0.03}_{-0.03}$	$126.4^{+17.6}_{-20.6}$	$22.6^{+1.0}_{-0.9}$	$-25.16^{+0.57}_{-0.58}$	1.05

Brassard, & Fontaine, 2020; Bergeron et al., 2011; Blouin, Dufour, & Allard, 2018; Holberg & Bergeron, 2006; Kowalski & Saumon, 2006; Tremblay, Bergeron, & Gianninas, 2011). While the photometry of 17 Dra A, B, and C agrees well with that expected for main-sequence stars, 17 Dra D is significantly fainter than main-sequence stars but appears much bluer than these stars. The photometry of this star corresponds to that of DA white dwarfs. We therefore conclude that 17 Dra is an evolved hierarchical quadruple star system with 17 Dra D, which is the former primary component of this system. 17 Dra D is the only white dwarf companion detected in the Gaia DR3 among the targets whose multiplicity is studied in this work. The remaining companions detected directly by Gaia around the targets are main-sequence stars, except for 57 CnC B, which, like its primary, is a giant star.

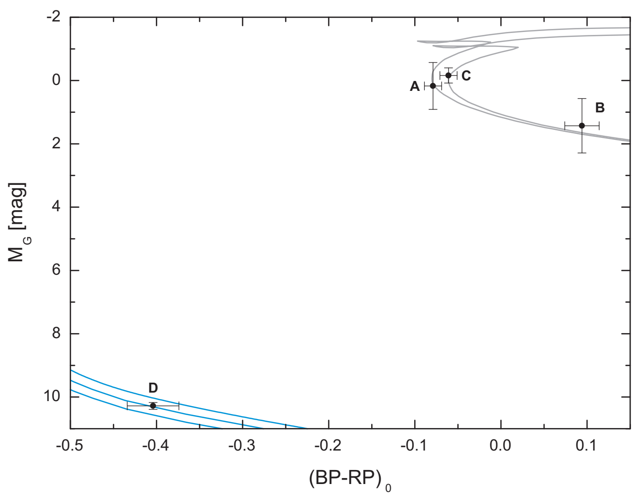

FIGURE 15 Color-magnitude diagram of all components of the 17 Dra system. The isochrones of stars with ages of 270 (left) and 310 Myr (right) are shown as gray lines, and the blue curves are the mass tracks of DA white dwarfs with masses of 0.6 (upper), 0.7 (middle) and 0.8 $M_\odot$ (lower). The photometry of 17 Dra A and its companions 17 Dra B and C agrees well with that expected for main-sequence stars. In contrast, the photometry of 17 Dra D corresponds to that of DA white dwarfs.

The RV of HD 148374 (RV $= -23.52 \pm 0.23$ km/s) remained stable throughout our 79-day spectroscopic monitoring period. Using data from the WDS and Gaia DR3, we classified the star as a binary system with a projected separation of approximately 140 au.

HD 169487 is listed in the WDS as a single star, but we identified a wide companion to the star in the Gaia DR3, with a projected separation of approximately 50200 au. Therefore, HD 169487 is the primary star of a wide binary system. During our 91-day spectroscopic monitoring of the star, its RV remained constant (RV $= 3.93 \pm 0.39$ km/s).

Using Gaia DR3 astrometry, we proved that 57 Cnc is a binary system with a projected distance of 180 au. The RV of the star remained constant during our spectroscopic observations (RV $= -57.68 \pm 0.28$ km/s).

γ And, which has a triple-star companion at a projected separation of approximately 1000 au, also exhibited a constant RV during our spectroscopic monitoring campaign (RV $= -57.68 \pm 0.28$ km/s).

HD 11031 is a quintuple star system. Its primary component is a binary system with an orbital period of approximately 37 years. There are two distant companions: HD 11031 B at a projected separation of approximately 270 au, which is a spectroscopic binary system itself, and HD 11031 C at a separation of about 2800 au. During our spectroscopic observation campaign, we investigated the RV of the primary component of this system, which exhibited a constant RV of (RV $= -4.48 \pm 0.59$ km/s).

κ And has a substellar companion located at a projected separation of about 50 au. No other companions of the star are listed in the Gaia DR3, and its RV remained constant (RV = −18.96 ± 1.86 km/s) during our spectroscopic study of the star.

λ Cas is a binary star system for which an orbital solution with a period of approximately 246 years was determined. The RV of the star remained constant during our spectroscopic monitoring program (RV = −19.18 ± 2.92 km/s).

7 Cr B is a hierarchical quintuple system. The two stars 7 CrB A and 7 CrB B have a projected separation from each other of approximately 990 au and were both observed with FLECHAS as part of our RV monitoring program. They both exhibit significant RV variations. 7 CrB A is an SB2 system with an orbital period of about 1.7 days. It also shows a linear trend in its periodic RV variation, indicating the presence of an additional companion in an orbit of a few au. In contrast, 7 CrB B is an SB1 system with an orbital period of about four days.

No companions are known for HD 214007, neither in the WDS nor in the Gaia DR3. During our RV monitoring program of the star, we found that HD 214007 is an eccentric ($e \sim 0.5$) SB1 system with an orbital period of about 10 days.

Our spectroscopic observations of the star ι Her revealed that its RV varies periodically. The best-fitting orbital solution for the star's RV data shows that it is an eccentric ($e \sim 0.5$) SB1 system with an orbital period of approximately 112 days. This star together with HD 214007 are the most eccentric binary systems identified in our spectroscopic monitoring program.

HD 201433 A has a wide companion located at a projected separation of about 410 au, which is listed in the Gaia DR3. The star also has a variable RV, but it was difficult to find an orbital solution that fits the RV data of the star well. The best-fitting orbital solution, which considers all RV measurements, has $\chi^2_{\rm red} = 7.78$, so it is not of acceptable quality. Since no linear trend in the RV residuals was observed as in 7 CrB A, the RV scatter of HD 201433 A was considered intrinsic. The conspicuous RV scattering of the star is also present in the SB9, where it is suggested that the star is a binary consisting of two pulsating variables. Assuming this to be the case, we removed the identified RV outliers to determine the system's best-fitting Keplerian orbital solution. It is worth noting in this context that the elements of the two determined solutions do not differ significantly. According to our orbital solutions, the star is an SB1 system with an orbital period of about 3.3 days, making HD 201433 a hierarchical triple star system at least.

For all stars with variable RV, we provide the mean and standard deviation of their RV measurements in Table 27. The RV standard deviation is at least one order of magnitude larger than the uncertainty of the systemic velocity resulting from Keplerian orbital fitting of these binary systems. This demonstrates that a sufficient number of RV measurements well covering the orbital phase of these binary systems is required to accurately determine their mean RV. This is crucial for precisely deriving the three-dimensional space velocity of these systems, which is necessary for accurately calculating their trajectory in the Milky Way.

TABLE 27 The mean and standard deviation of the RV measurements of all targets with significantly variable RV, compared to the determined systemic velocity γ of these binary systems. In the case of HD 201433 A, the results written in gray exclude some outliers, see Section 4.5 for details.

Target	$\overline{\rm RV}$ [km/s]	γ [km/s]
7 CrB Aa	-41.46 ± 79.17	$-30.79^{+0.66}_{-0.66}$
7 CrB Ab	-19.17 ± 76.92	$-30.79^{+0.66}_{-0.66}$
7 CrB B	-18.73 ± 4.87	$-18.43^{+0.50}_{-0.51}$
HD 214007	-21.19 ± 27.19	$-19.62^{+1.22}_{-1.23}$
ι Her	-22.64 ± 4.47	$-21.23^{+0.20}_{-0.20}$
HD 201433 A	-23.17 ± 15.62	$-23.57^{+1.47}_{-1.66}$
HD 201433 A	-26.91 ± 14.00	$-25.16^{+0.57}_{-0.58}$

All data recorded as part of our spectroscopic monitoring project is available from us upon request.

ACKNOWLEDGMENTS

We thank the observers at the University Observatory Jena who have contributed to some of the FLECHAS observations, in particular: L. Cortese, S. Hüttel, G. Paylı, and S. Emmerichs. This work has made use of data from the European Space Agency (ESA) mission *Gaia* (`https://www.cosmos.esa.int/gaia`), processed by the *Gaia* Data Processing and Analysis Consortium (DPAC, `https://www.cosmos.esa.int/web/gaia/dpac/consortium`). Funding for the DPAC has been provided by national institutions, in particular the institutions participating in the *Gaia* Multilateral Agreement. This research has made use of the SIMBAD database, as well as the VizieR catalogue access tool, CDS, Strasbourg, France. The original description of the VizieR service was published in Ochsenbein, Bauer, and Marcout (2000).

REFERENCES

Anderson, E., & Francis, C. (2012, May), *Astron. Lett.*, *38*(5), 331-346.

Bailer-Jones, C. A. L., Rybizki, J., Fouesneau, M., Demleitner, M., & Andrae, R. (2021, March), *AJ*, *161*(3), 147.

Bätz, J., Neuhäuser, R., Hambaryan, V. V., & Hambardzumyan, L. A. (2025), *A&A*.

Bédard, A., Bergeron, P., Brassard, P., & Fontaine, G. (2020, October), *ApJ*, *901*(2), 93.

Bergeron, P., Wesemael, F., Dufour, P. et al. (2011, August), *ApJ*, *737*(1), 28.

Blaauw, A. (1961, May), *Bulletin Astronomical Institute of the Netherlands*, *15*, 265.

Blouin, S., Dufour, P., & Allard, N. F. (2018, August), *ApJ*, *863*(2), 184.

Bressan, A., Marigo, P., Girardi, L., Salasnich, B., Dal Cero, C., Rubele, S., & Nanni, A. (2012, November), *MNRAS*, *427*(1), 127-145.

Carson, J., Thalmann, C., Janson, M. et al. (2013, February), *ApJ*, *763*(2), L32.

Castro-Ginard, A., Penoyre, Z., Casey, A. R. et al. (2024, August), *A&A*, *688*, A1.

Chen, Y., Bressan, A., Girardi, L., Marigo, P., Kong, X., & Lanza, A. (2015, September), *MNRAS*, *452*(1), 1068-1080.

Chen, Y., Girardi, L., Bressan, A., Marigo, P., Barbieri, M., & Kong, X. (2014, November), *MNRAS*, *444*(3), 2525-2543.

Drummond, J. D. (2014, March), *AJ*, *147*(3), 65.

Gaia Collaboration, Vallenari, A., Brown, A. G. A. et al. (2023, June), *A&A*, *674*, A1.

Hartkopf, W. I., Mason, B. D., & Worley, C. E. (2001, December), *AJ*, *122*(6), 3472-3479.

Holberg, J. B., & Bergeron, P. (2006, September), *AJ*, *132*, 1221.

Johnson, D. O. (2004, December), *Journal of Astronomical Data*, *10*, 3.

Kowalski, P. M., & Saumon, D. (2006, November), *ApJL*, *651*, L137.

Marigo, P., Girardi, L., Bressan, A. et al. (2017, January), *ApJ*, *835*(1), 77.

Mason, B. D., Wycoff, G. L., Hartkopf, W. I., Douglass, G. G., & Worley, C. E. (2001, December), *AJ*, *122*(6), 3466-3471.

Mugrauer, M. (2019, December), *MNRAS*, *490*(4), 5088-5102.

Mugrauer, M., Avila, G., & Guirao, C. (2014, January), *AN*, *335*(4), 417.

Mugrauer, M., Kollak, A.-K., Pietsch, L., & Michel, K.-U. (2025, June), *Astronomische Nachrichten*, *346*(5), e70005.

Ochsenbein, F., Bauer, P., & Marcout, J. (2000, April), *A&A,S*, *143*, 23-32.

Pastorelli, G., Marigo, P., Girardi, L. et al. (2020, November), *MNRAS*, *498*(3), 3283-3301.

Pastorelli, G., Marigo, P., Girardi, L. et al. (2019, June), *MNRAS*, *485*(4), 5666-5692.

Pourbaix, D., Tokovinin, A. A., Batten, A. H. et al. (2004, September), *A&A*, *424*, 727-732.

Tang, J., Bressan, A., Rosenfield, P., Slemer, A., Marigo, P., Girardi, L., & Bianchi, L. (2014, December), *MNRAS*, *445*(4), 4287-4305.

Tody, D. (1993, January), IRAF in the Nineties. In R. J. Hanisch, R. J. V. Brissenden, & J. Barnes (Eds.), Astronomical Data Analysis Software and Systems II Vol. 52, p. 173.

Tremblay, P.-E., Bergeron, P., & Gianninas, A. (2011, April), *ApJ*, *730*, 128.

Wenger, M., Ochsenbein, F., Egret, D. et al. (2000, April), *A&A,S*, *143*, 9-22.